Internally-cooled tools and cutting temperature in contamination-free machining

Carlo Ferri[a,b], Timothy Minton[a,*], Saiful Bin Che Ghani[a,c], Kai Cheng[a]

[a]*Brunel University, AMEE - Advanced Manufacturing and Enterprise Engineering, Kingston Lane, Uxbridge, Middlesex, UB8 3PH, UK*
[b]*Coventry University, Priory Street, Coventry, CV1 5FB, UK*
[c]*Universiti Malaysia Pahang, Lebuhraya Tun Razak, 26300 Gambang, Malaysia*

Abstract

Whilst machining heat is generated by the friction inherent into the sliding of the chip on the rake face of the insert. The temperature in the cutting zone of both the insert and the chip rises, facilitating adhesion and diffusion. These effects accelerate the insert wear, ultimately undermining the tool life. A number of methods have been therefore developed to control the heat generation. Most typically, metal working fluids (MWFs) are conveyed onto the rake face in the cutting zone, with negative implications on the contamination of the part. Many applications for instance in health-care and optics are often hindered by this contamination. In this study, microfluidics structures internal to the insert were examined as a means of controlling the heat generation. Conventional and internally-cooled tools were compared in dry turning of AA6082-T6 aluminium alloy in two 3^3 factorial experiments of different machining conditions. Statistical analyses supported the conclusion that the chip temperature depends only on the depth of cut but not on

*Corresponding author. Tel.: +44 1895 267945; fax: +44 1895 267583.
Email address: `timothy.minton@brunel.ac.uk` (Timothy Minton)

the feed rate nor on the cutting speed. They also showed that the benefit of cooling the insert internally increases while increasing the depth of cut. Internally-cooled tools can therefore be particularly advantageous in roughing operations.

Keywords: Cutting temperature, internally-cooled tool, contamination-free machining, dry machining

---

1. Introduction

The large amount of heat generated in the cutting zone whilst machining is in many cases detrimental to the performance of the cutting tool. The generated heat can have a serious impact on the quality of the machined parts, causing them to be re-worked or scrapped. In conventional tools, the heat conducted into the insert can in turn pass into the tool holder. The consequent increase in the temperature of the tool holder may have an effect on the dimensional accuracy of the machined surface[1]. Many authors state that a reduction of the cutting zone temperature through strategic heat transfer improves the tool life[2,3,4,5]. The notion of dousing the cutter and work-piece with cooling fluid was first reported as a beneficial technique by Taylor[6]. Many metal working fluids (MWFs) are hazardous to the operator and can cause respiratory and dermatological illnesses[7]. A number of studies have been carried out highlighting that between 7-17% of the cost for a manufactured part is related to the coolant and the associated treatment activities[2]. Great effort has been made to remove the coolant completely (dry machining)[2,3,4] or just to reduce the used amount (Minimum Quantity Lubrication, MQL)[3]. Removing flood cooling appears beneficial to the safeguard of the environment and of the machine operator health, while also providing a financial advantage to the manufacturer. However, the fundamental machining requirement to manage the temperature in the cutting zone must always be confronted. The potential hazards associated with high cutting temperatures can include tool failure, slowed production rates and geometrical inconsistency of the machined part leading to higher production cost[5].

The desirable end result of the removal of MWFs from metal cutting is the opportunity to carry out contamination-free machining. There may be applications where an external coolant supply has prohibitive contraindications. This would be for example the case when machining sensitive materials for optics or bio-medical applications or when machining harmful materials such as radioactive materials.

In dry contamination-free machining, the most significant issue is the elevated cutting temperatures hindering the tool life and thus increasing the production cost[2]. The aim of this investigation is to compare dry contamination-free machining with a conventional and with an internally-cooled tool to address the issue of raised cutting temperatures.

The shearing of material by the cutting tool generates a large amount of heat at the tool-chip interface[8]. Numerical models and simulations suggest temperatures at this interface can be as high as 400°C whilst machining aluminium alloys[9,10]. At these temperatures, specific microstructural changes occur[11]. According to Quan *et al*[12], between 60-95% of this heat is dissipated into the chips formed by the cutting process. High temperature in this region also creates a rapid formation of a Built-Up-Edge (BUE), where the work-piece material adheres to the surface of the tool making it blunt. BUE affects the quality of the part, increases forces and the cutting temperature. The complexities within the cutting region with regards to abrasion, adhesion and diffusion are also well documented[13,14]. Adhesion of the work-piece material to the tool is highly influenced by the temperature in the cutting zone[14,15]. Subsequent tool wear and BUEs cause additional heat generation. This cycle continues until the sharp edge of the tool can no longer effectively shear the material in the cutting zone. The tool ploughs in the work-piece compromising the surface finish of the part. Another detrimental but equally destructive wear mechanism is chipping/notching of the cutting edge. This can take place due to a rapid disconnection of the BUE[13]. The high temperature within the interface region must therefore be controlled. Abrasive wear is unavoidable in cutting as the process is essentially based on shearing the work-piece material. In effective management of the cutting temperature, the temperature should be reduced to a magnitude that minimises the degree of adhesive and diffusive wear.

New approaches to thermal control cover the application of non-traditional cooling media and the methods by which it is applied to the work-piece. Among these media, the usage of cryogenic coolants likes liquid nitrogen (N_2) and carbon dioxide (CO_2) has been reported. Among these methods, high pressure jet cooling has also been studied[16]. However, in all of these methods the coolant is a consumable and in most cases it is applied in an open loop system. For the cryogenic examples the coolant evaporates and cannot be collected and re-circulated.

A solution to this age-old problem is the notion of an internally-supplied coolant within a closed loop system. Such a system was first described in the seventies[17,18] and has then been attempted many times using a plethora of different designs and methods[19,20,21]. Fundamentally, a fluid is pumped though the tool shank, into a heat exchanger module situated beneath the cutting insert and back out through the tool shank. Channelling heat into the tooling may seem counter intuitive due to potential problems that this may cause (higher wear rates, diffusion, adhesion, tool expansion). But the internal fluid will enable the heat transfer from the cutting zone to an external heat sink much more quickly than the time needed for these potential problems to arise within the tooling.

Other researchers[22] advocate the addition of internal cooling to tool systems as a means of reducing the temperature of the cutting tool. Tungsten carbide is a relatively poor heat conductor, so the heat generated during cutting cannot readily be transferred through conventional tungsten carbide tools. The internal flow of coolant acts as an express way for the heat conducted from the tool-chip interface zone into the tool to an external heat sink.

As much as 95% of the heat generated during cutting has been reported to dissipate into the chip[12]. Measuring the temperature of the chip appeared therefore a sensible choice to establish the effect of cooling the tool internally. Any decrease of the measured chip temperature during cutting with the internally-cooled tool compared to conventional inserts would suggest that the internally-cooled tool is effective in transferring a significant fraction of the heat generated at the chip-rake face interface during cutting.

Many authors have attempted to measure the temperature within the cutting zone using an array of different techniques. The most popular of these is the embedded thermocouple[8]. This would be easy to implement using a standard monolithic cutting insert. However, in this investigation the internal geometry of the cooling structure makes this option not viable. The thermocouple is required to be as close to the cutting tip as possible. But the cooling channels are also required to be as close to the cutting tip as possible in order to maximise the effect of the internal coolant. There is a very large thermal gradient experienced during cutting and so a thermocouple which is placed more than a few millimetres from the tool tip will not give an accurate measurement of the cutting temperature. Another circumstance that would deter investigators from the use of embedded thermocouples is the change in the dynamics of heat transfer within the tool inserts caused by the thermocouple itself and the necessary hole[8,23]. Another method used in previous studies is the tool-work thermocouple or dynamic thermocouple[24]. This is difficult to use due to the relatively low electrical conductivity of the tungsten carbide inserts. In this study, a non-contact infrared pyrometer was used to measure the chip temperature. This method has been successfully used by previous studies to validate numerical and finite element analysis (FEA) models where the tool-chip interface temperatures have been calculated[25]. This method is deemed difficult to use due to the fluctuating emissivity of materials such as metals. However, once the pyrometer has been correctly calibrated using the black body technique, the measurements can be considered fairly reliable.

2. Experimental set up and cutting trials

The intent of testing dry cutting conditions led to the selection of a material for the test parts that can facilitate cutting operations. An aluminium alloy was considered because its machinability characteristics make the wear resistance properties of the insert, which is the central critical part of the set-up, less demanding. A reduced number of conventional and internally-cooled inserts was therefore needed than the number that would have been required in machining other materials, say for example steel. The aluminium alloy AA6082-T6 with relatively high silicon and magnesium content (0.7-1.3 and 0.6-1.2 % in weight, respectively) was selected due to its ready availability and widespread usage in several applications. One cylindrical bar was machined in cutting trials with a conventional tool insert and a second bar was instead machined in cutting trials with the internally-cooled tool. Diameter and length of the two AA6082-T6 blanks were 65 mm and 450 mm respectively. The length of the bar was sufficient to observe in each trials the establishment of a steady measured temperature of the chip surface. A minor drawback was that the high aspect-ratio of the blank required a tailstock to be used on the lathe. The cutting trials were performed using an Alpha Colchester Harrison 600 Group CNC lathe. In Figure 1, the machine set-up is displayed. In the figure the tool system, the work-piece and pyrometer used to measure the chip temperature are shown.

[Figure 1 about here.]

Internally-cooled tools were designed and manufactured by modifying commercially available tools. This approach greatly reduced the development time and cost. The designed internally-cooled cutting tool consists of three main components: *(a)* the modified cutting insert, *(b)* the cooling adaptor accommodating the micro channel and *(c)* the tool holder with the inlet and the outlet ports. A representative geometrical model of the modified cutting insert assembled onto the cooling adaptor is displayed in Figure 2.

[Figure 2 about here.]

The selected cutting insert was square in shape, without chip-breaker and made of tungsten carbide (WC) with 6% cobalt (SNUN120408, produced by Hertel). The insert was purpose-machined by electro-discharge machining (EDM) to fabricate a squared bottle-cap shape part with 1 mm wall thickness. It was then attached to the cooling adaptor in such a way that an empty cavity near the cutting zone is created between the insert and the adaptor. This cavity hosts the flow of coolant during operations. The cooling adaptor was machined on a five-axis micro-milling machine to accommodate ad hoc designed micro channels of 800 μm diameter to enable coolant recirculation inside the above-mentioned cavity. The module made of the insert and the cooling adaptor was then assembled with a tool holder. An off-the-shelf tool holder (CSBNR 2525M 12-4, produced by Sandvik) was modified so that inlet and outlet tubes for the internal-coolant could be fixed on the bottom and side surfaces, respectively. Figure 3 displays a production phase of the cooling adaptor on a five-axis micro-milling machine, the squared bottle-cap insert, the cooling adaptor and the assembled tool system.

[Figure 3 about here.]

The coolant used in the experiment was pure water with corrosion inhibitor which was pumped in a closed loop system by a micro diaphragm liquid pump (NFB 60 DCB made by KNF- Neuberger). The pump can deliver up to 1.2 L/min with twin heads which allows coolant speed to be varied and controlled.In this study, for simplicity the coolant speed was kept constant at 0.3 L/min.

The experimental set-up was complemented with a thermal sensor, a data acquisition system and a data processing software. The thermal sensor used in this study was a laser pyrometer with minimum spot size of the beam equals to 0.45 mm (μ-Epsilon, model CTLM3- H1 CF2). The pyrometer was fixed at 150 mm above the cutting insert and pointed to a single point on the insert's rake face about 1 mm away of the cutting edge (cf Figure 1). The temperature measurements were acquired at 1000 Hz and then transferred to a computer-based acquisition system. Dedicated software (Compact connect) provided by the pyrometer manufacturer enabled to display dynamically the measured temperature values. Also, in this software, the emissivity of the target surface could be set. In this study, the emissivity of the target surface has been determined as 0.78.

The values of the instantaneous chip temperatures recorded during all the cutting trials appeared to achieve a steady state condition. In the attempt of identifying unambiguously this state, a procedure has been devised. A unique value of temperature has then been associated with the identified steady state for each cutting trial. In this way, high reproducibility of the steady state temperature is assured. The procedure involved three stages. First, the start and the end of each machining operation were uniquely identified by recording the instants of time when the measured temperature exceed the minimum temperature measurable by the pyrometer (150 °C). Second, the interquartile range of the temperature distribution measured between the identified start and end was calculated. Third, the average of the temperatures measured within the interquartile range is computed and defined as the steady state temperature of the chip. Figure 4 illustrates the procedure. This steady state chip temperature measured during a machining trials is taken as representative of all the thermal information available about the trial performed in pre-specified, designed machining conditions.

[Figure 4 about here.]

3. Design of the Experiment

During machining operations with the internally cooled tool, the temperature (T) of the chip was measured in a set of experimental conditions identified by three controllable technological variables: the depth of cut (d), the feed rate (f) and the cutting speed (v). Due to their numerical nature, these variables have been considered as continuous rather than categorical. For each variable three values were considered identifying a region of interest in the space (d, f, v). Symbols, units and values of the technological variables are presented in Table 1.

[Table 1 about here.]

The number of the different experimental conditions (treatments) was therefore 3^3, i.e. 27. For each of the 27 treatments the cutting test was replicated three times, thus giving a total of 81 tests. The run order of the treatments was generated by assigning each of them a unique label and then randomly drawing a sequence of 27 labels from all the possible 27! label permutations. Once the machine was set up according to a specific treatment, all the three cutting tests for that treatment were performed. Changing from one experimental condition to another was a time consuming operation that prohibited to randomise fully the order of the 81 tests. If some nuisance event occurred while performing the three tests for a specific treatment, then its potential effect on the chip temperature would have been erroneously attributed to the treatment. However, the controlled conditions of the laboratory where the tests took place limited the likelihood for such random nuisance events to occur.

4. Modelling and Statistical Analysis

The main objective of this section is to construct a quantitative functional relationship (i.e. a model) between T and $(d,\ f,\ v)$ in a region of the three-dimensional technological space $(d,\ f,\ v)$.

In Figure 5, the 81 test results are grouped by depth of cut. To make the figure clearer, overlapping points at the same depth of cut were separated by adding a random small amount to each abscissa of the points (jittering procedure)[26]. The average chip temperature for each depth of cut is designated with a triangle, whereas the median with a square. Mean and median both suggest that the chip temperature increases linearly with the depth of cut. The boxplot with notches in the same figure further confirmed the initial graphical intuition.

[Figure 5 about here.]

For each group of data (i.e. for the Ts measured at one of the three depths of cut), each box is made of three horizontal segments, identifying the first quartile, the median and the third quartile of the Ts, respectively. two notches (i.e. two vertical 'v' with apexes ending on the median segment) are calculated and drawn at each side of the boxes. If the notches of two boxes do not overlap, the median of the two groups are significantly different at about 95 % confidence level[27]. The dashed vertical lines in the same figure (called whiskers) extend 1.5 times the value of the interquartile range. They are meant to identify values lying far apart from the majority of the data in a group. In Figure 5, it is noticed that there are three such points when $d = 0.5\,\text{mm}$. A further investigation did not highlight any assignable cause for the occurrence of these values. So these three experimental results where treated as unlikely but possible events. Thus, they were not excluded from the analysis.

In Figure 6, the chip temperatures have been grouped by feed rate and by cutting speed. Opposite to Figure 5, these boxplots do not suggest any significant difference in the median chip temperature when the feed rate is changed. Likewise, changing the cutting speed does not appear to affect T significantly. Five extreme points appears in the two boxplots of Figure 6. Yet, as before, further investigation did not reveal any assignable cause of their outlying. These points were therefore not excluded from the analysis. In the same figure, the variability of the chip temperature appears dubiously constant. In particular, the group of feed rate 0.1 mm/rev is of difficult interpretation due to the simultaneous presence of 3 extreme points and a noticeably small interquartile range relatively to the other groups.

[Figure 6 about here.]

No significant second order interaction effect of (d, f, v) on T was apparent in the examined interaction plots. To select a model to fit the data, a step-wise procedure with forward selection of the independent variables was followed[28]. Starting from the model with only the mean chip temperature and no variables included (also known as the null model), models with increasing complexity are considered by adding one variable at a time. When a variable is included, the p-value of the F-test assessing the significance of the decrease in deviance yielded by the inclusion is evaluated. If the reduction of deviance (i.e. the sum of the squares of the residuals alias the unexplained variation in the response variable) is statistically significant, then the corresponding technological variable is included into the model. Else, it is not (cf pages 323-329 in Crawley[26], with adjustments). Second degree terms of two variables are included in the model only if each of the single variables are per se significant (marginality restrictions)[29,28]. The results of the variable selection procedure are shown in Table 2. The calculations were performed with R, a language and environment for statistical computing[30].

[Table 2 about here.]

As a consequence of Table 2, the feed rate and the cutting speed are not included in the proposed statistical model, which is synthesised by the following equation:

$$T_i = \beta_0 + \beta_1 d_i + \epsilon_i \tag{1}$$

Equation 1 describes the expected chip temperature versus the depth of cut as a straight line. The index $i = 1, 2 \ldots, 81$ identifies each of the actual cases in the data available. The terms ϵ_i are random variables that, without losing generality, are assumed to be independent and identically distributed with mean zero and constant variance σ^2. If they are also normal, further analysis of the model parameters are facilitated. The 2+1 parameters (β_0, β_1 and σ) have been estimated with the ordinary least-squares method (OLS) using the functions available in R[30]. A more complex model including a quadratic term in the depth of cut was also considered, namely: $T_i = \beta_0 + \beta_1 d_i + \beta_1 d_i^2 + \epsilon_i$. As shown in Table 3, the model with the second degree term in d (i.e. d^2) does not lead to a significant reduction of the unexplained variation of the response, when compared with the straight-line model (p-value=9.6 %). Thus the term d^2 is excluded from equation 1.

[Table 3 about here.]

The model of equation 1 was tested for lack of fit[28]. From a practical point of view, this means that If $\hat{\sigma}$ for the model is not significantly larger than the estimated repeatability standard deviation of the temperature measurement procedure, then the assumption that the model fits the data cannot be rejected. The results of the tests are displayed in Table 4. A p-value=9.62 % shows that the lack of fit is not significant. The estimated repeatability standard deviation of the chip temperature measuring procedure equals 16.3 °C $\left(\sqrt{\frac{20792}{78}}\,^{\circ}\mathrm{C}\right)$, whereas the estimated standard deviation of the errors is 16.5 °C $\left(\sqrt{\frac{21548}{79}}\,^{\circ}\mathrm{C}\right)$.

[Table 4 about here.]

Graphically, the test for lack of fit shows that the difference between the fitted and the mean points for each of the cutting depths tested is not significant (cf the X and the triangular points in Figure 5).

The estimated intercept and slope are displayed in Table 5 together with their estimated standard deviations (i.e. standard errors).

[Table 5 about here.]

The differences between the measured temperature values and the corresponding predictions of the model (fitted values) are referred to as residuals. If the errors ϵ_i are independent and with equal variance, then the residuals should not exhibit any pattern nor varying scatter, regardless of how they may have been grouped. In Figure 7 the residuals are displayed versus the fitted temperature values and versus the depth of cut (both jittered). The group means are also displayed as triangular points (there are 3 groups of 27 data points in each of the two diagrams).

[Figure 7 about here.]

Figure 7 raises the suspicion that the variance of the errors is not constant. The residuals with larger fitted values appear to have lower dispersion than the others. Due to the proportionality of the fitted temperature and the depth of cut (cf equation 1), the residuals also appear to have lower variation when the depth of cut is larger (Figure 7). New models were therefore considered to account for heteroscedastic errors (cf the classes of variance functions in the R package *nlme*[31,32]). The exponential variance function (i.e. `varExp()`) offered the best fitting of the model to the data in terms of Akaike Information Criterion (AIC)[32]. The variance of the errors is modelled by this class as described in the following equation:

$$\mathrm{Var}\,(\epsilon_i) = \sigma_a^2 e^{2\,\delta\,d_i} \tag{2}$$

In equation 2, σ_a and δ are two parameters in the model that are estimated using the restricted maximum likelihood method (REML) as implemented in the `gls()` function of `nlme`. The estimates are displayed in Table 6 together with approximate 95 % confidence intervals for the same estimated parameters.

[Table 6 about here.]

The difference of the intercepts and the slopes in the two models does not appears significant. The corresponding confidence intervals overlap (cf Tables 5 and 6). Yet Figure 8 shows that equation 2 successfully accounts for the variance structure of the errors.

[Figure 8 about here.]

Similar analyses have been performed on data collected in designed machining trials with an uncooled tool in the same experimental conditions. These analyses led to the same conclusion that only the depth of cut is a significant explanatory variable for the the chip temperature. The fitted model can be described with the same terms present in Equation 1. The OLS estimates of the model parameters and their 95 % confidence intervals under the hypothesis of normally distributed errors are displayed in Table 7.

[Table 7 about here.]

The confidence intervals of the intercept and the slope of the model for the internally-cooled tool do not overlap with the corresponding confidence intervals calculated for the conventional tool (cf Table 6 and 7) . This is a strong evidence that the internal microfluidics structures are effective in changing the measured thermal characteristics of the chip.

Opposite to the case of the cutting trials with the internally cooled tool, in Figure 9 the residuals do not exhibit any pattern of variance increasing with the depth of cut (Figure 7).

[Figure 9 about here.]

5. Practical implications of the findings

The Analysis in the previous section provides quantitative evidence that for the internally-cooled tool the dispersion of the temperature measurement results is decreasing while depth of cuts and chip temperatures increase (cf. Figure 7). A possible reason can be identified in the measuring system of the chip temperature. The diameter of the pyrometer laser beam was in fact 0.45 mm. So when measuring the chip temperature, if the width of the chip is smaller than 0.45 mm, the part of the laser beam that exceeds the size of the chip may hit upon part of the tool rake face. If this interpretation holds, then for depth of cut less than 0.45 mm the chip temperature measurements may be biased.

The potential bias in measuring the temperature may be the reason why the straight lines in Figure 10 intersect. These continuous and dashed lines in Figure 10 represent the models fitted to the the experimental results from the cutting trials with an internally-cooled and a conventional tool, respectively. A possible different interpretation of the intersection between the two lines is that the internally-cooled tool is indeed effective in reducing the chip temperature only beyond a critical depth of cut. Further investigation outside the scope of this investigation is required to clarify this point.

[Figure 10 about here.]

This constantly varying exposed area of the rake face to the laser beam may be the cause of the inflated variability of the errors at lower depth of cut. However, it has been shown above that the changed structures of the errors variance does not affect significantly the OLS estimates of the intercept and of the slope of the model.

This consideration may also help to explain the rather unexpected circumstance that at $d = 0.20$ mm six measured chip temperature values obtained with the internally cooled tool are higher than any other temperature measured when machining at the same depth of cut with a conventional tool (Figure 10).

The same set-up for measuring the temperature has been used also in the experiment with a conventional tool not internally cooled. Yet, in that case no reduced dispersion of the temperature measurement results was observed when increasing the depth of cut (cf. Figure 9). The suspicion may thus arise that the increased fluctuation of temperature at small depths of cut may be a typical characteristic of the material removal mechanism with an internally cooled tool. Further study would be needed to support this intuition.

The observation of Figure 10 does however remove any doubt that at $d = 0.50$ mm an internally-cooled turning tool is significantly effective in reducing the chip temperature. The extrapolation (cf Crawley[26], page 412) of the two models of Figure 10 to depths of cut larger than 0.50 mm supports the speculative expectation that the internally-cooled cutting tool is increasingly effective in reducing the chip temperature.

6. Conclusions

This study aimed at exploring the thermal characteristic of cutting processes with a purpose-built, internally-cooled prototype of a tool system. Chip temperature in turning of AA6082-T6 aluminium alloy with conventional and internally-cooled turning tools were compared in two separated 3^3 factorial experiments in the space of the technological variables depth of cut, cutting speed and feed rate. No external coolant was used in the machining trials.

Linear statistical models with homoscedastic and heteroschedastic errors were fitted to the experimental results. OLS and REML methods were respectively used to estimate the parameters of the fitted models.

The statistical analyses showed that the measured chip temperature appears to depend significantly only on the depth of cut but not on the feed rate nor on the cutting speed.

These analyses also suggest that, as the depth of cut is increased, the internally-cooled tool is incrementally more effective in reducing the chip temperature than the conventional tool is. Consequently, when no MWFs are used, internally-cooled tools appear to be potentially advantageous over conventional tool in roughing operations.

In cutting trials with internally-cooled tools, a significantly increased fluctuation of the chip temperature has been identified when decreasing the depth of cut.

Acknowledgements

This research was performed within the scope of the collaborative research project 'Self-learning control of tool temperature in cutting processes'(ConTemp) funded by the European Commission 7th Framework Programme (Contract number: NMP2-SL-2009-228585). The authors gratefully acknowledge the committed support of all the technical staff in the AMEE Department at Brunel University. Particular gratitude goes to Mr Paul Yates for his help in the cutting trials.

Abbreviations

AIC Akaike information criterion

BUE Built-up edge

EDM Electro-discharge machining

FEA Finite element analysis

MQL Minimum Quantity Lubrication

MWF Metal working fluid

OLS Ordinary least squares

REML Restricted maximum likelihood

References

[1] S. Carvalho, S. Lima e Silva, A. Machado, G. Guimares, Temperature determination at the chiptool interface using an inverse thermal model

considering the tool and tool holder, Journal of Materials Processing Technology 179 (13) (2006) pp. 97 – 104.

[2] F. Klocke, G. Eisenblaetter, Dry cutting., CIRP Annals - Manufacturing Technology 46 (2) (1997) pp. 519 – 526.

[3] P. S. Sreejith, N. B. K. A., Dry machining: Machining of the future., Journal of Materials Processing Technology 101 (13) (2000) pp. 287 – 291.

[4] K. Weinert, I. I., J. W. Sutherland, T. Wakabayashi, Dry machining and minimum quantity lubrication., CIRP Annals - Manufacturing Technology 53 (2) (2004) pp. 511 – 537.

[5] G. Byrne, D. Dornfeld, D. Berend, Advancing cutting technology, CIRP Annals - Manufacturing Technology 52 (2) (2003) pp. 483 – 507.

[6] F. W. Taylor, On the art of cutting metals, American Society of Mechanical Engineer 28 (29 1119) (1907) pp. 31–350.

[7] D. I. Bernstein, Z. L. Lummus, G. Santilli, S. James, L. I. Bernstein, Machine operator's lung. a hypersensitivity pneumonitis disorder associated with exposure to metalworking fluid aerosols., Chest 108 (1) (1995) pp. 636–641.

[8] M. J. Longbottom, L. J. D., Cutting temperature measurement while machining a review., Aircraft Engineering and Aerospace Technology 77 (2) (2005) pp. 122 – 130.

[9] C. Dinc, I. Lazoglu, A. Serpenguzel, Analysis of thermal fields in orthogonal machining with infrared imaging, Journal of Materials Processing Technology 198 (13) (2008) pp. 147 – 154.

[10] I. Lazoglu, Y. Altintas, Prediction of tool and chip temperature in continuous and interrupted machining, International Journal of Machine Tools and Manufacture 42 (9) (2002) pp. 1011 – 1022.

[11] G. E. Trotten, S. D. Mackenzie, Handbook of Aluminum: Vol. 1: Physical Metallurgy and Processes, CRC Press, 2003.

[12] Y. Quan, Z. He, Y. Dou, Cutting heat dissipation in high-speed machining of carbon steel based on the calorimetric method., Frontiers of Mechanical Engineering in China 3 (2) (2008) pp. 175–179.

[13] M. Nouari, G. List, F. Girot, D. Coupard, Experimental analysis and optimisation of tool wear in dry machining of aluminium alloys, Wear 255 (712) (2003) pp. 1359 – 1368.

[14] H. Takeyama, N. Iijima, Y. Yamamoto, Experimental analysis and optimisation of tool wear in dry machining of aluminium alloys, CIRP Annals - Manufacturing Technology 36 (1) (1987) pp. 421 – 424.

[15] H. Takeyama, N. Iijima, Y. Yamamoto, Tool/chip adhesion and its implications in metal cutting and grinding, International Journal of Machine Tool Design and Research 14 (4) (1974) pp. 335 – 349.

[16] E. M. Trent, P. K. Wright, Metal Cutting, 4th Edition, Butterworth-Heinemann, Oxford, 2000.

[17] N. P. Jeffries, R. Zerkle, Thermal analysis of an internally-cooled metal-cutting tool, International Journal of Machine Tool Design and Research 10 (3) (1970) pp. 381 – 399.

[18] N. P. Jeffries, Internal cooling of metal-cutting tools, Industrial Lubrication and Tribology 24 (4) (1972) pp. 179 – 181.

[19] J. C. Rozzi, J. K. Sanders, W. Chen, The experimental and theoretical evaluation of an indirect cooling system for machining, Journal of Heat Transfer 133 (3) (2011) 1–10.

[20] H. Zhao, G. C. Barber, Q. Zou, R. Gu, Effect of internal cooling on tool-chip interface temperature in orthogonal cutting, Tribology Transactions 49 (2) (2006) pp. 125–134.

[21] L. E. A. Sanchez, V. L. Scalon, G. G. C. Abreu, Cleaner cleaner machining through a toolholder with internal cooling, in: Advances in Cleaner Production, no. 3, Universidade Paulista, 2011, pp. pp. 125–134.

[22] E. Uhlmann, M. Roeder, E. Fries, F. Byrne, Internal cooling of cutting tools, in: International Conference and Exhibition on Laser Metrology, Machine Tool, CMM and Robotic Performance, no. 9, Laser metrology and machine performance IX : 9th International Conference and Exhibition on Laser Metrology, Machine Tool, CMM & Robotic Performance, LAMDAMAP 2009, 2009, pp. pp. 215–223.

[23] A. A. Tay, A review of methods of calculating machining temperature, Journal of Materials Processing Technology 36 (3) (1993) pp. 225 – 257.

[24] D. OSullivan, M. Cotterell, Temperature measurement in single point turning, Journal of Materials Processing Technology 118 (13) (2001) pp. 301 – 308.

[25] M. Davies, T. Ueda, R. M'Saoubi, B. Mullany, A. Cooke, On the measurement of temperature in material removal processes, CIRP Annals - Manufacturing Technology 56 (2) (2007) pp. 581 – 604.

[26] M. Crawley, The R book, Wiley, 2007.

[27] R. McGill, J. W. Tukey, W. A. Larsen, Variations of box plots, The American Statistician 32 (1) (1978) pp. 12–16.

[28] J. J. Faraway, Linear Models with R, 1st Edition, Texts in Statistical Science, Chapman & Hall/CRC, 2004.

[29] W. N. Venables, B. D. Ripley, Modern Applied Statistics with S, 4th Edition, Springer, New York, 2002.

[30] R Development Core Team, R: A Language and Environment for Statistical Computing, R Foundation for Statistical Computing, Vienna, Austria (2011).

[31] J. Pinheiro, D. Bates, S. DebRoy, D. Sarkar, R Development Core Team, nlme: Linear and Nonlinear Mixed Effects Models, r package version 3.1-103 (2012).

[32] J. C. Pinheiro, D. M. Bates, Mixed-Effects Models in S and S-Plus, Springer, 2000.

List of Figures

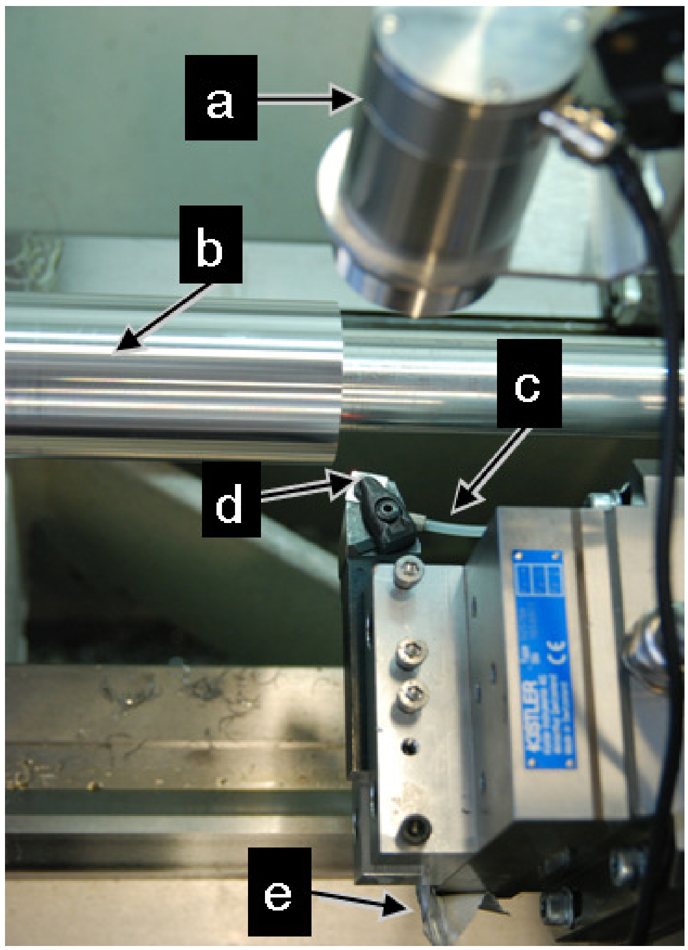

Figure 1: Experimental set-up of the internally-cooled tool on the CNC lathe: (a) pyrometer, (b) work-piece, (c) coolant outlet, (d) cutting tool, (e) coolant inlet.

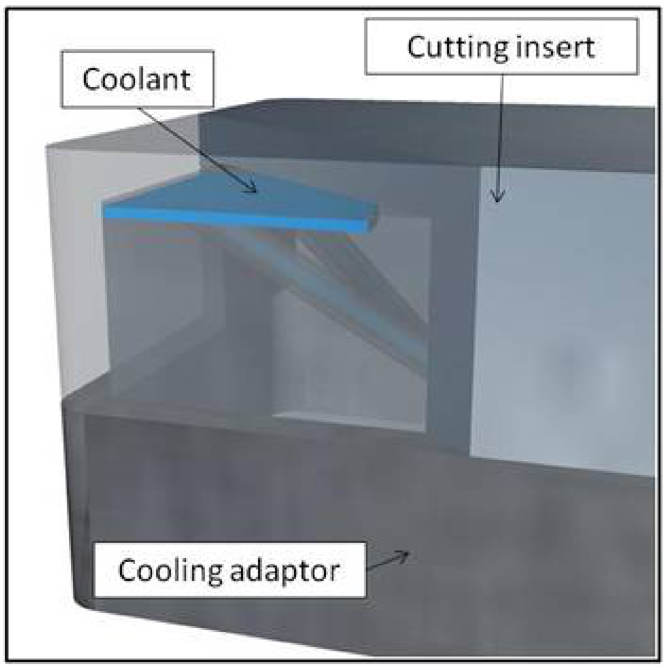

Figure 2: Bottle-cup-shaped and squared cutting insert assembled onto the cooling adaptor. The transparent corner of the insert makes the internal pool of coolant and the micro channels in the adaptor visible.

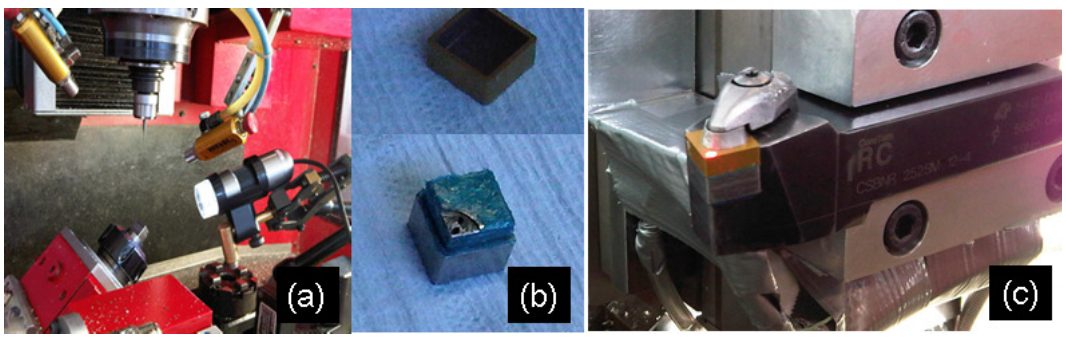

Figure 3: (a) Production of the micro channels in the cooling adaptor on a five-axis micro-milling machine; (b)top: bottle-cap insert, bottom: cooling adaptor; (c) fully integrated cutting tool.

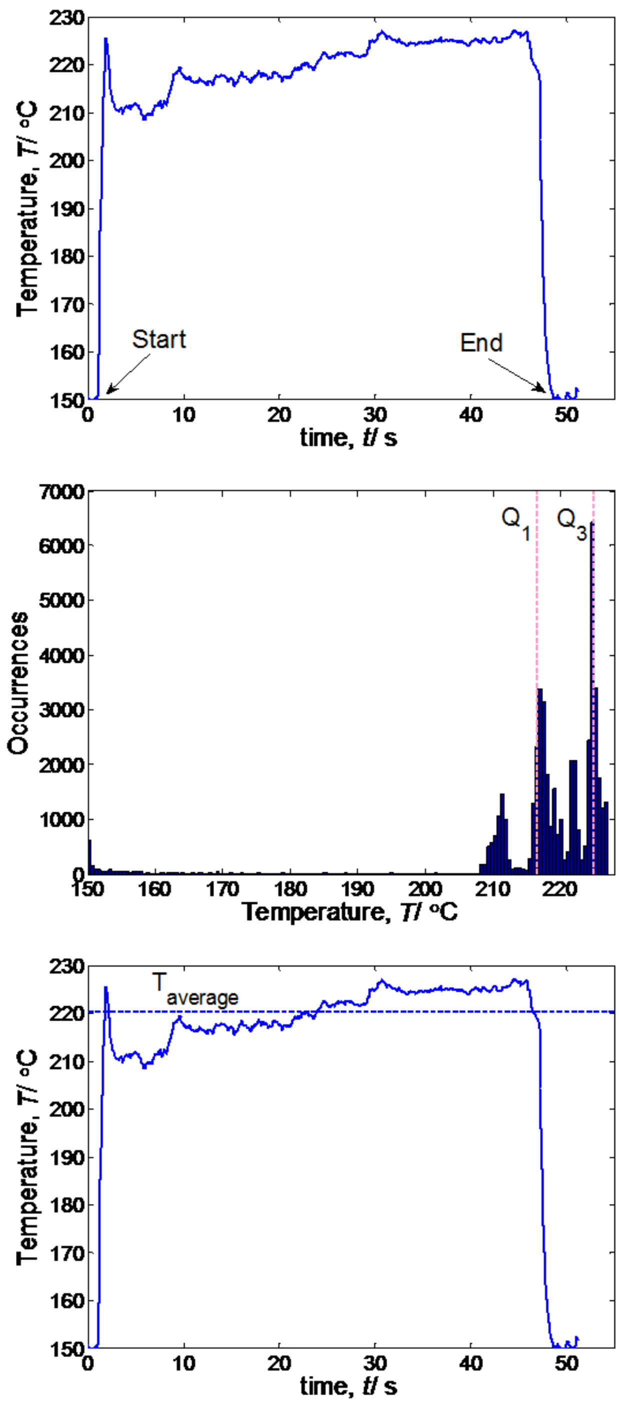

Figure 4: The three stages of the procedure to define the steady state chip-temperature.

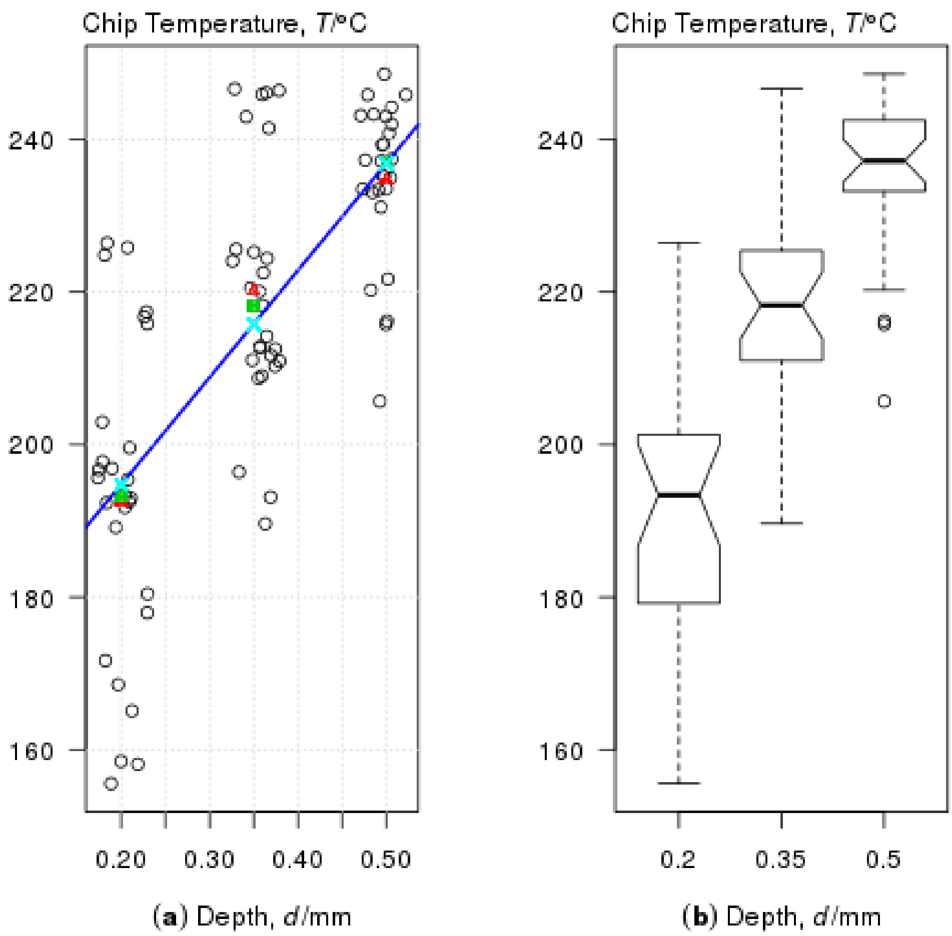

Figure 5: Chip temperature versus depth of cut (a) and its box plot representation (b).

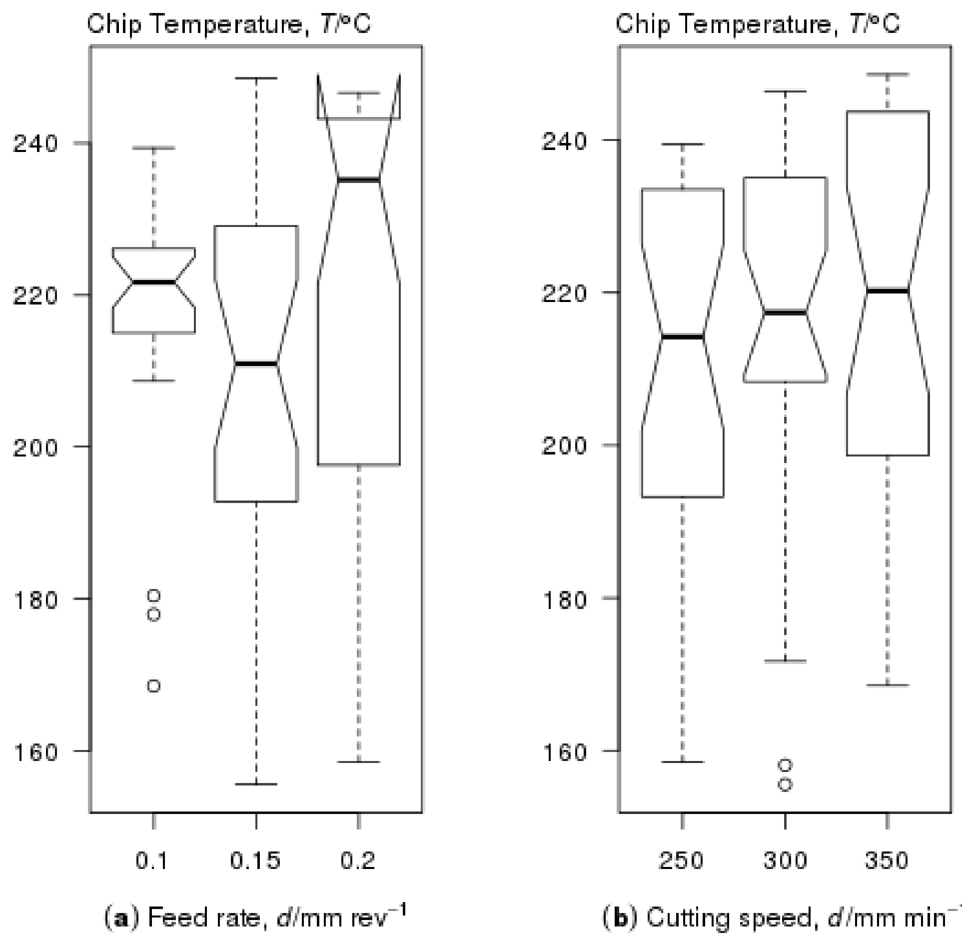

Figure 6: Boxplot of the chip temperature grouped by feed rate (a) and by cutting speed (b).

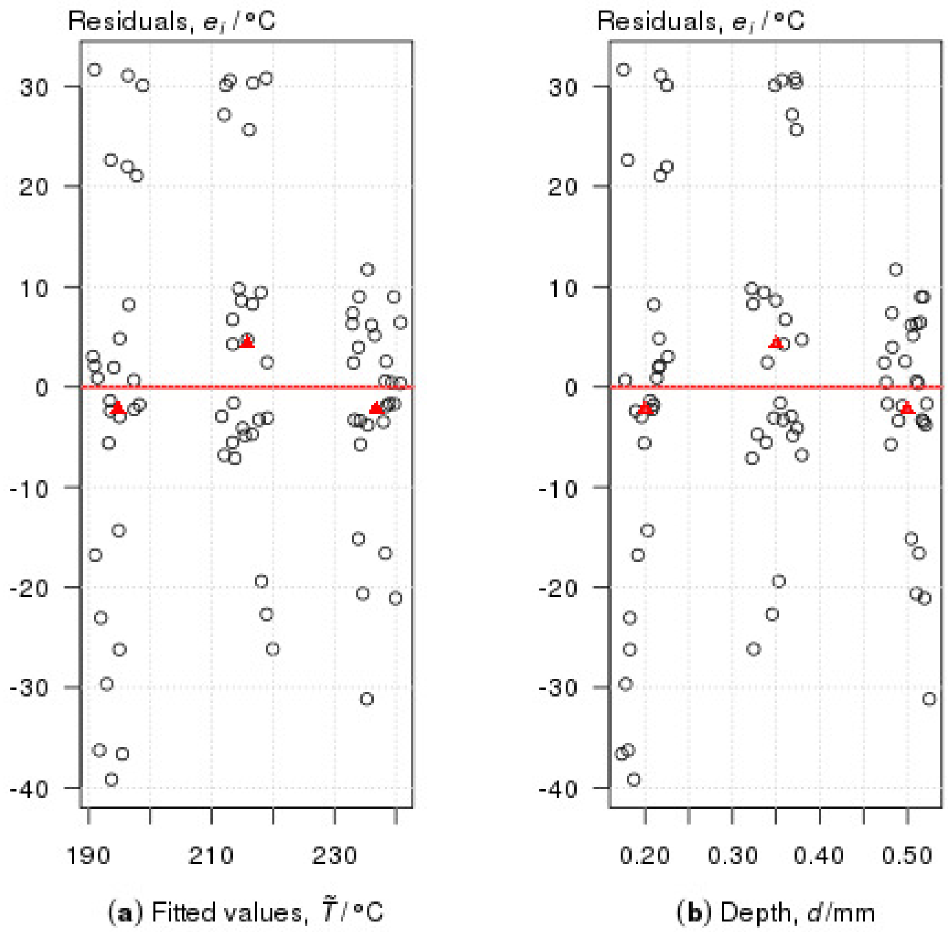

Figure 7: Residuals of the model in equation 1 against fitted values (a) and depth of cut (b).

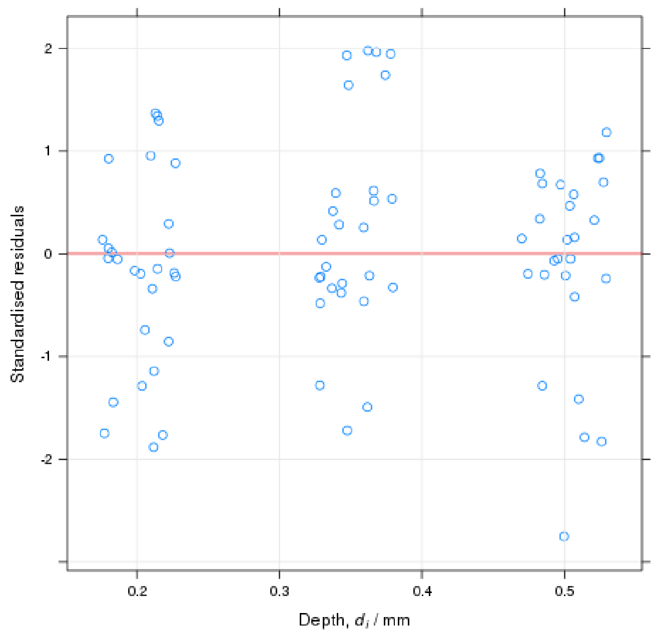

Figure 8: Standardised residuals of the model with variance of the errors varying according equation 2.

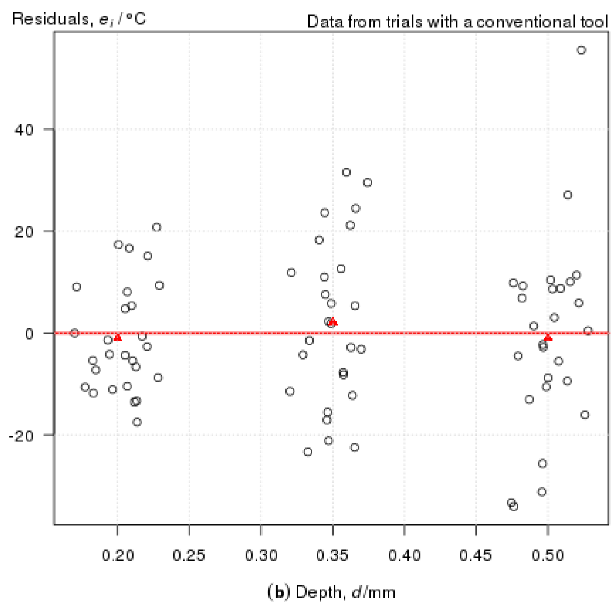

Figure 9: Residuals against depth of cut for the model fitted to the data from the trials with an uncooled tool.

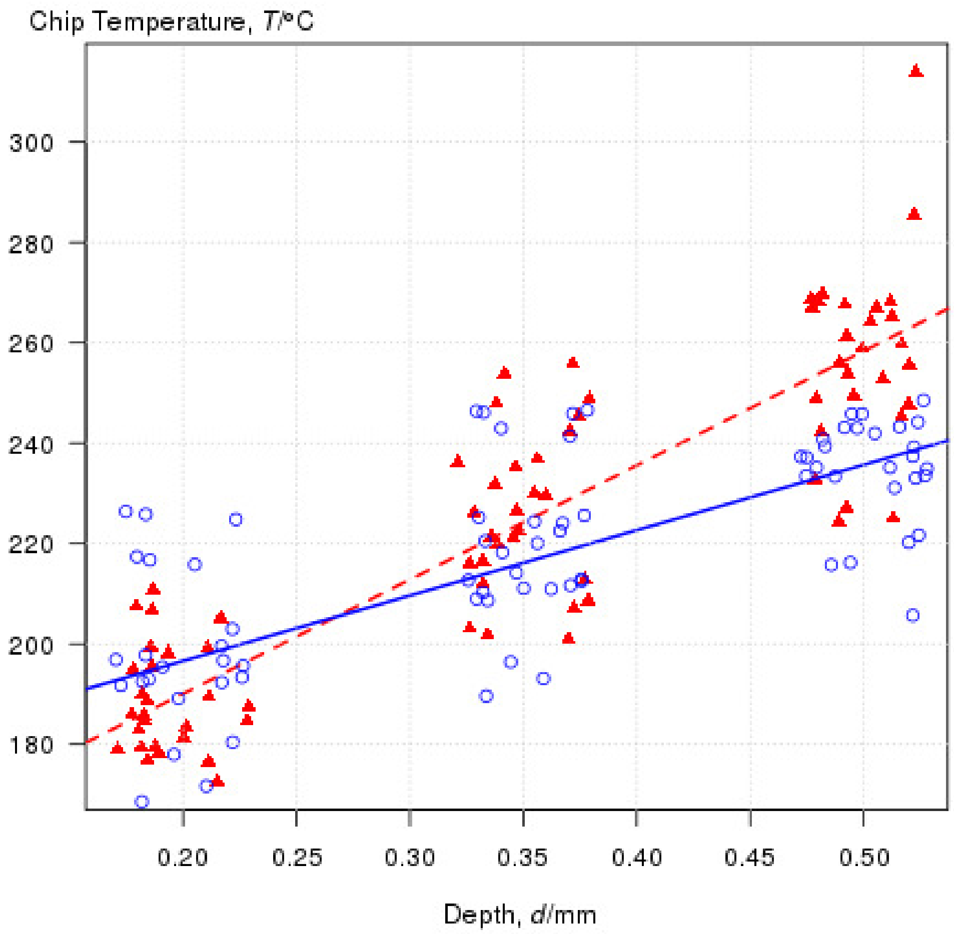

Figure 10: Chip temperature for the internally cooled and conventional turning tool against depth of cut. The temperatures are shown as round-shaped and triangle-shaped points respectively. The continuous and the dashed lines represent the fitted models in the two respective machining conditions.

List of Tables

Table 1: Technological variables and their levels.

Variable	Unit	values
depth of cut, d	mm	0.20, 0.35 and 0.50
feed rate, f	mm/rev	0.10, 0.15 and 0.20
coolant flow rate, r	L/min	0.00 and 0.30
cutting speed, v	mm/min	250, 300 and 350

Table 2: Selection of the technological variables to include in the model (Df= degrees of freedom, Sum Sq= sum of squares, Mean Sq= Mean of squares).

	Df	Sum Sq	Mean Sq	F-value	p-value
Depth	1	23927	23927.0	87.72	0.0000
Residuals	79	21548	272.8		
Feed	1	127	127.46	0.22	0.6388
Residuals	79	45347	574.01		
Speed	1	323	323.34	0.57	0.4542
Residuals	79	45151	571.53		
Depth	1	23927	23927	87.13	0.0000
Feed	1	127.46	127.46	0.46	0.4977
Residuals	78	21420	274.62		
Depth	1	23927	23927	87.93	0.0000
Speed	1	323.34	323.34	1.19	0.2790
Residuals	78	21224	272.10		

Table 3: Comparison of the first and the second degree models (Res Df= residuals degrees of freedom, RSS= residuals sum of squares, Df=Degrees of freedom).

	Res.Df	RSS	Df	Sum of Sq	F-value	p-value
1	79	21548				
2	78	20792	1	755.64	2.83	0.0962

Table 4: Test for lack of fit (Res Df= residuals degrees of freedom, RSS= residuals sum of squares, Df=Degrees of freedom, first row regression model, second row saturated model).

	Res.Df	RSS	Df	Sum of Sq	F-value	p-value
1	79	21548				
2	78	20792	1	755.64	2.83	0.0962

Table 5: OLS estimates of the parameters in the linear model with constant error variance. 95% confidence intervals of the parameters under the hypothesis of normally distributed errors are also displayed.

parameter	lower	estimate	upper
β_0 / °C	155.6	$\hat{\beta}_0 = 166.7$	177.7
β_1 / °C/mm	110.5	$\hat{\beta}_1 = 140.3$	170.1
σ / °C	14.29	$\hat{\sigma} = 16.52$	19.56

Table 6: REML estimates of the parameters in the extended linear model with error variance exponentially varying. Approximate 95 % confidence intervals of the parameters are also displayed.

parameter	lower	estimate	upper
$\beta_{a,0}$ / °C	158.1	$\hat{\beta}_{a,0} = 170.5$	182.9
$\beta_{a,1}$ / °C/mm	101.5	$\hat{\beta}_{a,1} = 130.4$	159.2
δ	-3.659	$\hat{\delta} = -2.309$	-0.9586
σ_a / °C	21.03	$\hat{\sigma}_a = 34.57$	56.84

Table 7: OLS estimates of the parameters in the linear model fitted to the data from the trials with an uncooled tool . 95 % confidence intervals of the parameters assuming normally distributed errors are also displayed.

parameter	lower	estimate	upper
$\beta_{u,0}$ / °C	134.1	$\hat{\beta}_{u,0} = 144.5$	154.9
$\beta_{u,1}$ / °C/mm	199.6	$\hat{\beta}_{u,1} = 227.6$	255.7
σ_u / °C	13.45	$\hat{\sigma}_u = 15.54$	18.40